

# Assessment of Corona with Partial Discharge and Radio Interference Measurement Circuits

Elena-Denisa Burada <sup>\* †</sup>, Mihaela Popescu <sup>\*</sup>, Tania Nicoară <sup>†</sup>, Viorica Voicu <sup>†</sup> and Ionel Dumbravă<sup>†</sup>

<sup>\*</sup> University of Craiova, Faculty of Electrical Engineering, Craiova, Romania,  
safta.elena.i4n@student.ucv.ro, mpopescu@em.ucv.ro

<sup>†</sup> National Institute for Research Development and Testing in Electrical Engineering, Craiova, Romania,  
tnicoara@icmet.ro, cem@icmet.ro, iodum@icmet.ro

**Abstract** - The paper presents how the physical phenomenon, corona discharge, can be assessed using circuits for measuring partial discharges (PD) and radio disturbances. In test circuits for PD measurement, corona discharges may also be present as a disturbing element at certain test voltages, even if all measures are taken to avoid them.

The main features and differences between the PD measurement circuit and radio interference voltage measurement circuit are presented, which include the measurement systems and their calibration methods. So for the PD measurement are presented calibration of the PD circuit with the same impulse charge but using different type of filters at PD instrument (wideband and narrowband). For the radio interference voltage measurement is presented calibration of the test circuit with the same voltage but with using different frequencies at the electromagnetic interference receiver.

In a test circuit simulating the occurrence of corona discharges, corona discharges were evaluated at different test voltages using the same measurement frequencies for the two systems. Differences were observed between the results obtained with the same measurement frequencies for the two systems, differences that were maintained regardless of the measurement system used.

The UV spectrum and the electric field of these discharges are correlated with the applied voltage. To assess the corona discharges, the electric field generated by these discharges at the highest test voltages was also measured.

**Cuvinte cheie:** descărcări corona, perturbații radio, sisteme de măsurare.

**Keywords:** corona discharge, radio disturbances, measurement systems.

## I. INTRODUCTION

Corona performance is one of the more important criterion when it comes to the design and construction of a transmission line. The high voltages at which modern transmission lines operate have increased the corona problem to the point to which they have become a concern to the power industry.

Consequently, these lines are now designed, constructed and maintained so that during dry conditions they will operate below the corona-inception voltage, meaning that the line will generate a minimum of corona-related phenomena. In foul weather conditions, however, water droplets, fog and snow can produce corona discharges [1].

One of the consequences of transmission line corona discharges is radio interference. Radio interference is a rather general term, which, by definition, refers to any unwanted disturbance within the radio frequency band, such as undesired electric waves in any transmission channel or device. This is also known as radio noise. Pulses of current and voltage are produced on transmission line conductors by corona discharges, which are pulsating in nature.

These pulses are characterized by rise and decay-time constants, in the order of a few nanoseconds to tens or hundreds of nanoseconds, and by repetition rates, which may be in the MHz range.

As a result of this, the frequency spectrum of these pulses can cover a considerable portion of the radio frequency band.

The electromagnetic fields resulting from the corona discharges may, therefore, create unwanted disturbances in the operation of a transmission channel or device over a wide range of frequencies [2].

While the radio disturbance (radio noise) from a high voltage overhead power lines may be established only by site measurement, for the line equipment and other high voltage equipments, laboratory measurements of the radio interference voltage are foreseen.

Now, the evaluation of radio disturbances including corona discharges can be done by two methods corresponding to the IEC 60270 standard dedicated to partial discharge (PD) measurements [3] and CISPR TR 18-2 dedicated to methods for measuring radio disturbances [4].

From this perspective, the common element of the standards can be considered as quasi-peak (QP) detector used, however, in measuring systems with different characteristics. Even if the IEC 60270 standard has been significantly improved (ed.3.1 of 2015) it has kept the use of radio interference meters of quasi-peak (QP) type for the measurement of partial discharges, although this meter can have different readings for the impulses with the same charge but different pulse repetition rate.

The CISPR TR 18-2 and QP detector has become part of electromagnetic compatibility (EMC) tests for radio interference voltage (RIV) test on high voltage equipment.

Below, circuits and measuring systems specific to the measurement of partial discharges (including corona discharges characteristic of the external insulation of high voltage equipment) according to IEC 60270 and CISPR TR 18-2 standards will be presented.

## II. MEASUREMENT OF PARTIAL DISCHARGES

Partial discharge measurement carried out in accordance with IEC 60270 has become an essential tool for quality assurance of high voltage equipment. The main objective of IEC 60270 is to standardize and unify the measurement of partial discharges in order to obtain comparable results for tests performed in different locations, with different equipment and by different operators.

To achieve this objective, IEC 60270 has defined a set of key processes and parameters that must be carefully followed [3].

The corona discharges being a particular case of partial discharges, which occur in gaseous media around conductors. The occurrence of PD generates small amplitude impulse current with very small rise and fall times (usually in the ns- $\mu$ s range, depending on the insulating medium).

The frequency range of such a pulse basically contains the high frequency HF (up to 10 MHz), very high frequency VHF (up to 200 MHz) and ultra-high frequency UHF (above 200 MHz) range [5].

Principle parameter for PD evaluation is the apparent charge  $q$ , whose amplitude (pC) is obtained by integrating the detected current pulses.

It is achieved using the PD measurement system with its input impedance  $Z_{mi}$  [3]: coupling device (CD), transmission system (connecting cable CC) and measuring instrument (MI) by means of a coupling capacitor  $C_k$  connected in parallel with the tested object with  $C_a$  capacitance (Fig. 1).

An extra component of the circuit presented in figure 1 is the filter characterized by a high impedance ( $Z$ ) at the measuring frequency to attenuate the radiofrequency currents in both direction, from the power supply used for generate the test voltage ( $U$ ) to the test circuit and from the test circuit to the power supply.

Through the coupling device the input currents are converted into output voltage signals which are transmitted to the measuring instrument via the connecting cable.

The MI that processes the PD signals captured at the terminals of the tested object are either analogue, equipped with an electronic integrator, or digital with direct A/D conversion of the input PD pulses and then their digital integration or A/D conversion after the integration of the input PD pulses has been performed through a band-pass filter.

According to the standard IEC 60270, the PD measurement instrument uses two types of pass filters: wide-band (bandwidth 100 kHz – 900 kHz, upper frequency max. 1 MHz) and narrow-band (midband frequency 50 kHz – 1 MHz, bandwidth 9 kHz – 30 kHz) [3].

No matter which measuring instrument you use, it is necessary to calibrate the measuring system in the complete test circuit by injecting from a calibrator connected to the terminals of the test object, current pulses proportional to the value of the injected charge (Fig. 2).

The calibrators consist of a generator that produces step voltage pulses of amplitude  $U_0$  in series with a capacitor  $C_0$ , so that the calibration pulses are repetitive charges, each with amplitude  $q_0 = U_0 C_0$ .

In practice it is not possible to produce ideal step voltage pulses. Although other waveforms with longer rise times  $t_r$  (10% to 90% of the peak value) and finite decay times  $t_d$  (90% to 10% of the peak value) can inject virtually the same charge value, the response of different measuring systems or test circuits may be different due to the integration error caused by the increased duration of these current pulses.

Therefore the parameters (Fig. 3) which characterize the step voltage used by the calibrator must satisfy the following conditions: rise time ( $t_r \leq 60$  ns), time to steady state ( $t_s \leq 200$  ns), step voltage duration ( $t_d \geq 5$   $\mu$ s), amplitude deviation of step voltage  $U_0$  between  $t_s$  and  $t_d$  ( $\Delta U \leq 0,03 U_0$ ).

The time parameters are measured from the origin  $t_0$  of the step voltage, which refers to the point in time when the voltage value is equal to 10% of  $U_0$ .

Time to steady state  $t_s$  is the shortest time during which the deviation  $\Delta U$  from the voltage  $U_0$  remains first time less than 3%.

Step voltage duration  $t_d$  is the time after  $t_s$  at which the step voltage amplitude drops below 97% of  $U_0$ . After  $t_d$ , the voltage must fall continuously below 10%  $U_0$  within a time interval greater than 500  $\mu$ s (Fig. 3).

Figure 2 shows the calibration in a PD measuring circuit with PD measuring system in series with  $C_k$ :  $U$  is the high voltage from the power supply,  $G$  is the step voltage generator of the calibrator,  $C_0$  is the capacitor of the calibrator with his stray capacitance  $C_s$ ,  $Z_{mi}$  is the input impedance of the PD measuring system, CC is the cable,  $C_a$  is the object under test,  $C_k$  is the coupling capacitor and CD is the coupling device.

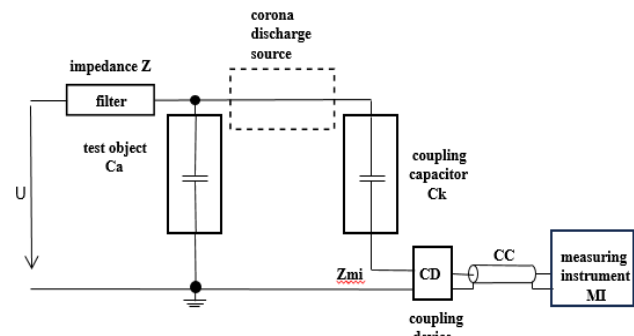


Fig. 1. PD measuring circuit.

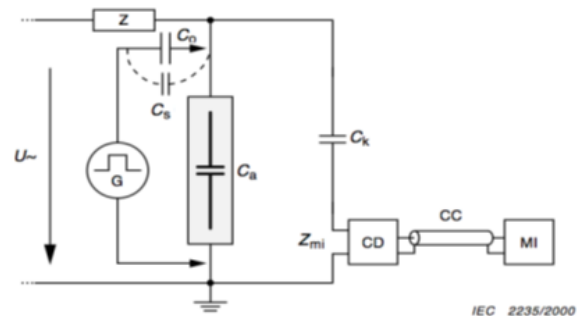


Fig. 2. Calibration in a PD measuring circuit with PD measuring system in series with  $C_k$ .

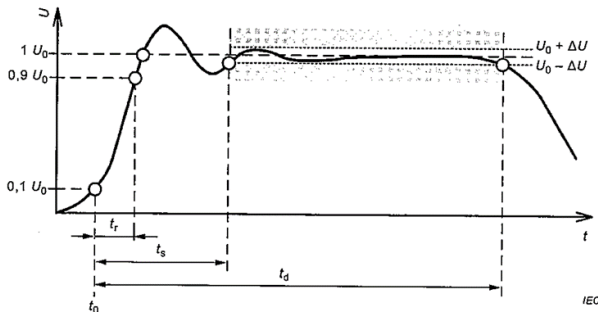


Fig. 3. The step voltage parameters of a calibrator.

The circuit presented in figure 1 was calibrated with 5 pC using a PD calibrator [9], which respects the parameters presented above.

The calibrator injects into the circuit (Fig.2) charge pulses of 5 pC with a pulse repetition frequency of 50 Hz. Different filters of the PD measuring system were used to acquire the charge pulses, wide-band filter (bandwidth 100 kHz – 900 kHz) and narrow-band filters (midband frequency 500 kHz and 1000 kHz with 9 kHz bandwidth). Figures 4 and figure 5 show the 5 pC pulse acquired by the PD measuring system with a wide-band filter (bandwidth 100 kHz – 900 kHz). At the top of each figure, the 5 pC pulse is presented on 20 ms (2 ms/div.) to visualize the partial discharges over a period of the power voltage applied in the circuit. This is useful for phase-resolved PD patterns obtained during any PD measurement (Fig. 4). The shape of this pulse is presented in figure 4 in the time domain, 500 μs/div. and in figure 5 is presented the frequency spectrum of this charge pulse used for calibration of the PD test circuit highlighting the bandwidth of the filter (Fig. 5).

In the same conditions, narrow-band filters of the PD measuring system were used, 500 kHz ± 4.5 kHz and 1000 kHz ± 4.5 kHz. Thus, figures 6 and figure 7 show the same 5 pC pulse acquired with a 500 kHz ± 4.5 kHz filter at PD measuring system (Fig. 6, Fig. 7).

Since it is the same PD pulse from the calibrator with a low pulse repetition frequency, no significant difference of the PD measuring system scale factors was observed for the selected frequency domains.

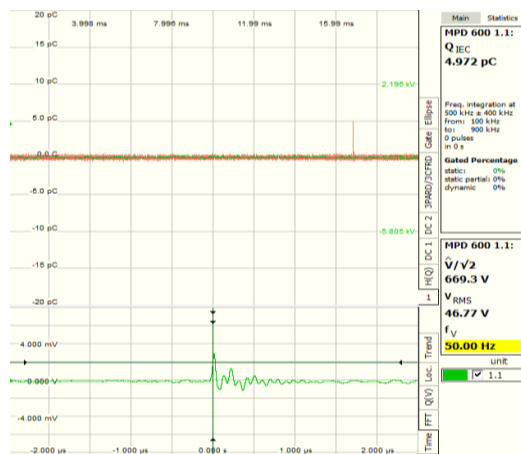


Fig. 4. PD measuring circuit calibration with 5 pC pulse and 500 kHz ± 400 kHz filter at PD measuring system.

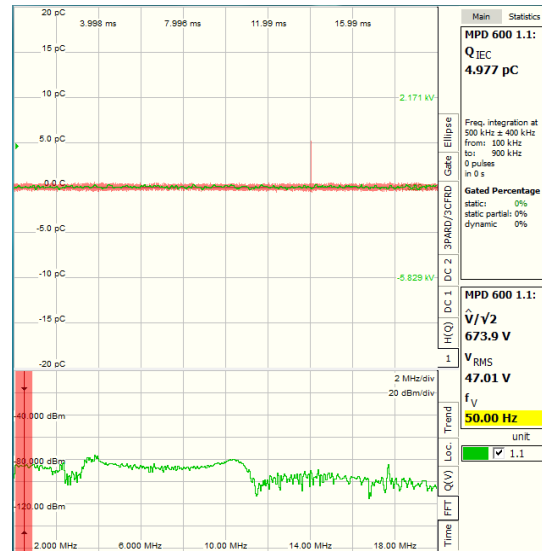


Fig. 5. Frequency spectrum of 5 pC pulse (500 kHz ± 400 kHz filter at PD measuring system).

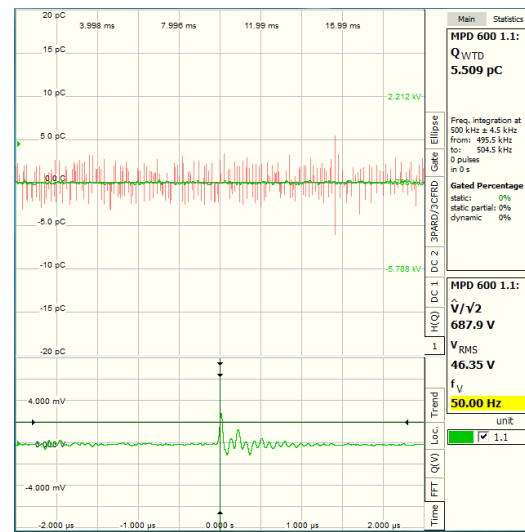


Fig. 6. PD measuring circuit calibration with 5 pC and 500 kHz ± 4.5 kHz filter at PD measuring system.



Fig. 7. Frequency spectrum of 5 pC pulse (500 kHz ± 4.5 kHz filter at PD measuring system).

### III. RADIO INTERFERENCE VOLTAGE MEASUREMENT

The measurement method according to the reference standard TR CISPR 18-2 TR CISPR 18-2 [4] can be used to measure the level of radio interference of high voltage equipment.

The main element of this measuring method is the measuring impedance,  $(300 \pm 40) \Omega$ , formed by the coupling capacitor  $C_k$  of 1nF and the resistance  $R_L$  (equivalent resistance of  $R_2$  in series with the parallel combination of resistance  $R_1$  and the input resistance  $R_i$  of the EMI receiver). To calculate the level of radio interference at different test voltages it is necessary to calibrate this test circuit.

For the calibration, a sine wave generator and a 20 k $\Omega$  resistor connected in series with the generator are used in order to inject a current of about 50  $\mu$ A into the test circuit according to the CISPR standard. Calibration of the radio interference voltage measuring circuit shall be performed to account for the inherent attenuation of such a circuit.

As a consequence the attenuation ( $A$ ) shall be calculated as the difference between the receiver EMI indications when injecting 1  $V_{RMS}$  from a sine wave generator at a measurement frequency of 1 MHz or 500 kHz between the test object terminal and ground when the test object is disconnected from the test circuit and when it is connected to the test circuit.

Since this value is obtained from the calculation by injecting the same sinusoidal voltage values at the same measurement frequency, this contribution does not affect the measurement uncertainty.

The radio interference voltage level is obtained using the formulas [4]:

$$V = V_m + A + R \quad (\text{dB}\mu\text{V}), \quad (1)$$

where:

$V_m$  - value measured during the test (dB $\mu$ V);

$A$  - test circuit attenuation:

$$A = A_2 - A_1 \quad (\text{dB}\mu\text{V}) \quad (2)$$

$A_1$  - EMI receiver reading obtained when calibrating the test object connected in the test circuit;

$A_2$  - EMI receiver reading obtained when calibrating the test object disconnected from the test circuit;

$R$  - correction factor with measurement resistance value,  $R_L$ ,

If  $R_2 = 275 \Omega$  and  $R_1 = R_i = 50 \Omega$  (Fig. 8), then  $R_L = 300 \Omega$  and

$$R = 20 \log(300/(50/2)) = 20 \log(600/(50)) = 21.6 \text{ dB}\mu\text{V} \quad (3)$$

The two values  $A$ ,  $R$  are basically constants which are added to the value measured at the EMI receiver during the test at different values of the test voltage.

For the circuit shown in figure 8 the  $A$  values obtained at the two measuring frequencies 500 kHz and 1000 kHz are the same, even if the  $A_1$  and  $A_2$  values measured at the two measuring frequencies are different. Thus  $A = 5 \text{ dB}\mu\text{V}$  can be considered for both measurement frequencies.

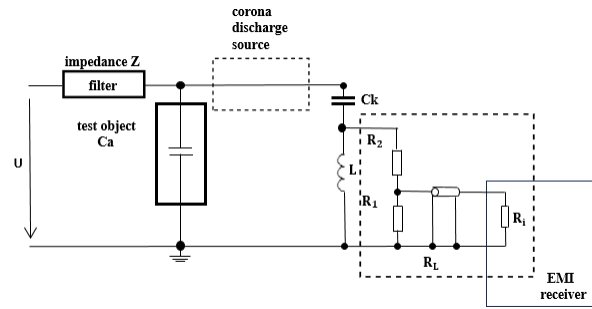


Fig. 8. RIV measuring circuit.

That is because the standards for high-voltage equipment, insulation strings and accessories used in the power transmission system specify permissible levels of radio interference voltage in  $\mu$ V, the value  $V$ , obtained in dB $\mu$ V, is converted to  $\mu$ V.

### IV. PRACTICAL MEASUREMENT AND COMPARISON OF PD AND RIV MEASUREMENT

The corona discharges were simulated using the test circuit shown in figure 9, and a specialized video camera equipped with a visible spectrum channel and a UV channel, with a sensitivity to detect radio interferences of min. 22 dB $\mu$ V at 1 MHz, was used to highlight the sources of corona discharges (Fig. 10).

Modern UV channel optical properties allow detection of ultraviolet radiation (wavelengths between 200-400 nm) emitted by the corona discharge, even in broad daylight, without being influenced by sunlight.

Corona discharges were assessed using a PD measurement system [6] which has the capability of histogram acquisition, oscilloscope-like visualization of an acquired signal and Fourier transform of this signal.

For the comparison, the narrow-band filters of the PD measuring system were used, 500 kHz  $\pm$  4.5 kHz and 1000 kHz  $\pm$  4.5 kHz. The results obtained at different test voltages, under the conditions of calibrating the test circuit with 5 pC, are shown in Table I [7].



Fig. 9. Test circuit for corona discharge simulation.

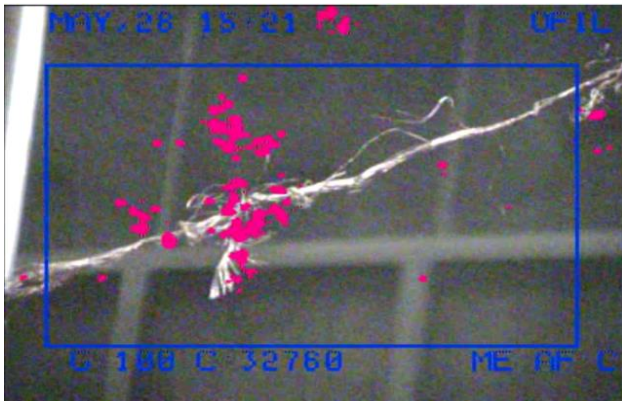


Fig. 10. Sources of corona discharges in the test circuit.

TABLE I.  
PD MEASUREMENT AT TWO MEASURING FREQUENCIES

Voltage (kV)	PD level (pC)	
	500 kHz ± 4.5 kHz	1000 kHz ± 4.5 kHz
80	350	460
70	320	450
60	310	330
50	300	250
40	220	210
30	140	150
20	110	110

Where the measurement frequency is used of 500 kHz ± 4.5 kHz, figure 11 shows the entire test sequence with PD patterns at 80 kV test voltage.

PD measurement system use, figure 12 show a corona discharge pulse visualized in the time domain and its frequency spectrum.

If a measurement frequency is used of 1000 kHz ± 4.5 kHz, figure 13 shows the entire test sequence with PD patterns captured at the same test voltage (80 kV).

Figure 14 show a corona discharge pulse visualized in the time domain and its frequency spectrum.

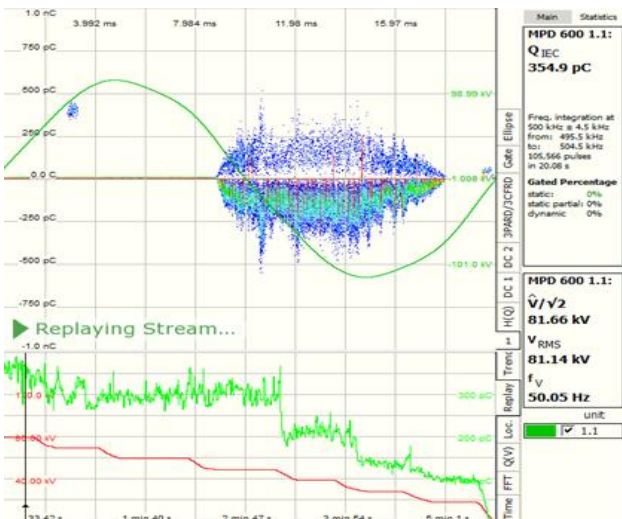


Fig. 11. PD patterns at test voltage 80 kV for the measurement frequency of 500 kHz ± 4.5 kHz.

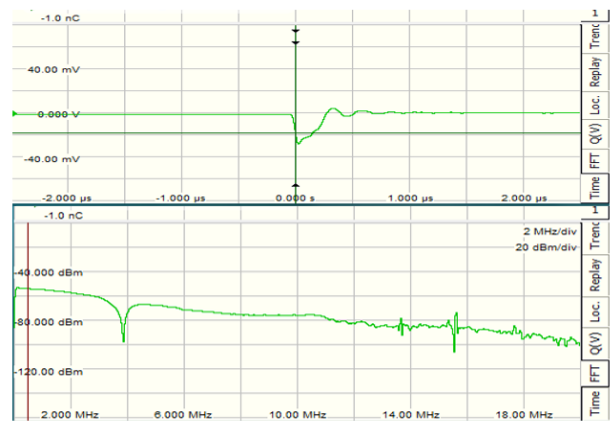


Fig. 12. PD pulse in time domain (up) and his frequency spectrum (down) measured at 80 kV test voltage for the measurement frequency 500 kHz ± 4.5 kHz.

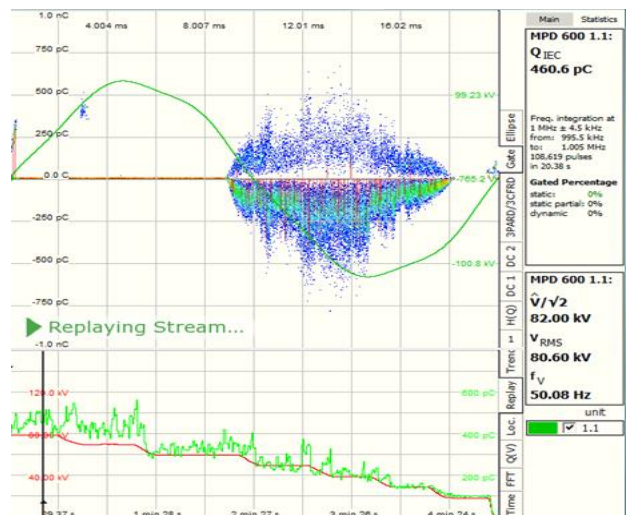


Fig. 13. PD patterns at test voltage 80 kV for the measurement frequency of 1000 kHz ± 4.5 kHz.

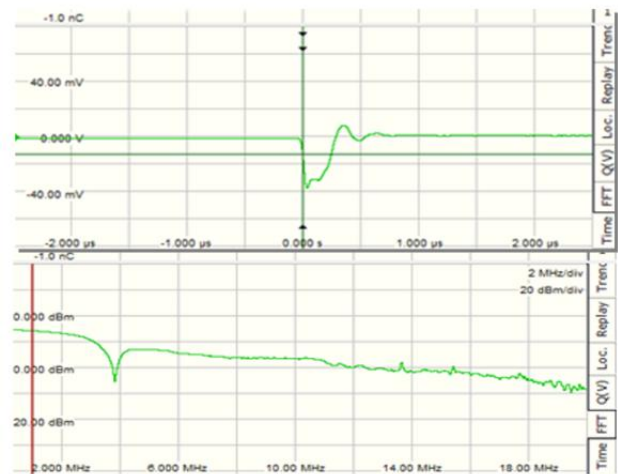


Fig. 14. PD pulse in time domain (up) and his frequency spectrum (down) measured at 80 kV test voltage for the measurement frequency 1000 kHz ± 4.5 kHz.

Therefore when calibrating the test circuit (5 pC) no differences were observed between the scale factor of the measuring system at the two measurement frequencies, the actual measurement showed a higher measured PD level at the measurement frequency of 1000 kHz  $\pm$  4.5 kHz for the higher test voltages (Table I, Fig. 11 and Fig. 13).

Experimental results using the RIV measuring system, at the same measurement frequencies, are presented in Table II. Calibration of the test circuit was carried out according to the method presented in Section III and no differences were observed between the circuit attenuation values determined at the two measurement frequencies. Higher RIV levels were also observed at the measurement frequency of 1000 kHz  $\pm$  4.5 kHz for higher test voltages.

TABLE II.  
RIV MEASUREMENT AT TWO MEASURING FREQUENCIES

Voltage (kV)	RIV level ( $\mu$ V)	
	500 kHz $\pm$ 4.5 kHz	1000 kHz $\pm$ 4.5 kHz
80	602.55	1071.52
70	537.03	758.57
60	478.63	676.08
50	358.92	638.21
40	269.15	426.57
30	229.08	327.34
20	213.79	213.79

To evaluate the corona discharges, the electric field generated by these discharges at the highest test voltages was also measured, using the EHP-50F field probe mounted at a height of 1m, a distance of 2.6 m from the vertical plane of the discharge source and the NBM-550 analyser (Fig. 15), with the results shown in Table III [10].



Fig. 15. Circuit for electric field assessment.

TABLE III.  
ELECTRICAL FIELD MEASUREMENT

Frequency [Hz]	Voltage [kV]	Measured electric field [kV/m]
50	80	5.789
	70	4.988
	50	3.543

The measured electric field was less than 10 kV/m limit (AL action trigger value according to Tab. B1 of Directive 2013/35/EU).

The limit is the AL value – “action levels (AL)” means operational levels set in order to simplify the process of proving compliance with the relevant ELV or, where appropriate, to take the relevant protective or preventive measures specified by Directive 2013/35/EU.

“Exposure limit values (ELVs)” means values established on the basis of biophysical and biological considerations, in particular on the basis of short-term and scientifically proven direct effects, i.e. thermal effects and electrical stimulation of tissues.

“ELV for health effects” means exposure values above which workers could be exposed to adverse health effects such as thermal heating or stimulation of nerve or muscle tissue.

“ELV for sensory effects” means exposure values above which workers could be exposed to temporarily disturbed sensory perceptions and temporary minor changes in brain functions [8].

Taking into account the above, the measured electric field does not have a harmful effect on the workers' health.

## V. CONCLUSIONS

This paper presents how to evaluate corona discharges using different methods and measurement systems. Based on a laboratory test circuit simulating the occurrence of corona discharges, differences between the measured values at the standardized measurement frequencies 500 kHz  $\pm$  4.5 kHz and 1000 kHz  $\pm$  4.5 kHz could be observed for both measurement systems used.

This is because even if the two measurement circuits used have common elements, each of them has particularities that differentiate them, from the impedances of the measurement systems to the calibration methods of the circuits and that are reflected in the way the results are reported.

PD measurement system, which provides more information about the analysed phenomenon, indicated that there is a difference in PD pattern taking into account that the measurements were performed successively and not simultaneously.

The corona discharges were also evaluated from the point of view of the electric field generated which was below the electromagnetic field exposure limit value.

The phenomenon is important to study for configurations close to those used in the design of high voltage equipment and analysis in terms of electric field generated by discharges.

## ACKNOWLEDGMENT

This work was developed with funds from the Ministry of Research, Innovation and Digitization of Romania as part of the NUCLEU Program PN 23 33 01 02.

Contribution of authors:

First author – 50%

First coauthor – 20%

Second coauthor – 10%

Third coauthor – 10%

Fourth coauthor – 10%

Received on September 12, 2024

Editorial Approval on December 2, 2024

#### REFERENCES

- [1] Z. Wu, Q. Zhang, Z. Pei and H. Ni, "Correspondence between phase resolved partial discharge patterns and corona discharge modes," in *IEEE Transactions on Dielectrics and Electrical Insulation*, vol. 26, no. 3, pp. 898-903, June 2019.
- [2] P. Lukes, M. Clupek and V. Babicky, "Discharge filamentary patterns produced by pulsed corona discharge at the interface between a water surface and air," in *IEEE Transactions on Plasma Science*, vol. 39, no. 11, pp. 2644-2645, Nov. 2011.
- [3] IEC 60270:2015, "High-voltage test techniques - Partial discharge measurements," ed.3.1, 2015.
- [4] CISPR TR 18-2, "Radio interference characteristics of overhead power lines and high-voltage equipment", ed.3.0, 2017.
- [5] CIGRE, TF 15.11/33.03.02 "Knowledge rules for partial discharges diagnosis in service", April 2003.
- [6] Omicron "MPD 600 partial discharges measurement and analysis system".
- [7] E. -D. Burada, M. Popescu, T. Nicoară, V. Voicu and I. Dumbravă, "Evaluation of corona in partial discharge and radio interference measurement circuits," *2024 International Conference on Applied and Theoretical Electricity (ICATE)*, Craiova, Romania, 2024, pp. 1-5.
- [8] Directive 2013/35/EU of the European Parliament and of the Council of 26 June 2013 on the minimum health and safety requirements regarding the exposure of workers to the risks arising from physical agents (electromagnetic fields) (20th individual Directive within the meaning of Article 16(1) of Directive 89/391/EEC) and repealing Directive 2004/40/EC.
- [9] \*\*\*<https://www.megger.com/en-ca/products/cal1-cal2-and-cal3-calibration-impulse-generators>
- [10] \*\*\*<https://www.narda-sts.com/en/products/emf-selective-measuring-devices/ehp-50>